Chapter 5
Squeeze Film Bearing Characteristics for Synovial Joint Applications

T. V. V. L. N. Rao, Ahmad Majdi Abdul Rani and Geetha Manivasagam

Nomenclature

B	Width of parallel plate, m
C	Partial journal bearing radial clearance, m
h, H	Film thickness, m; $H = h/h_o$ for parallel plate; $H = h/C$ for partial journal bearing
h_o	Reference film thickness, m
k_1, K_1	Permeability of porous layer in region I, m^2; $K_1 = k_1/h_0^2$ for parallel plate; $K_1 = k_1/C^2$ for partial journal bearing
L	Length of parallel plate; length of partial journal bearing, m
p	Pressure distribution, N/m^2; $P = ph_0^3/\mu L^2(-\mathrm{d}h/\mathrm{d}t)$ for parallel plate, $P = pC^2/\mu R^2(\mathrm{d}\varepsilon/\mathrm{d}t)$ for partial journal bearing
q, Q	Flow rate (volume) per unit length, m^2/s; $Q = q/L(-\mathrm{d}h/\mathrm{d}t)$ for parallel plate; $Q = q/RC(\mathrm{d}\varepsilon/\mathrm{d}t)$ for partial journal bearing
R	Journal radius, m
u_i, U_i	Fluid velocity in surface (or porous) layer region I, couple stress fluid film region II, surface layer region III, respectively, m/s; U_i =

T. V. V. L. N. Rao (✉)
Department of Mechanical Engineering, SRM Institute of Science and Technology, Kattankulathur 603203, India
e-mail: tvvlnrao@gmail.com

A. M. A. Rani
Department of Mechanical Engineering, Universiti Teknologi PETRONAS, 32610 Seri Iskandar, Malaysia
e-mail: majdi@utp.edu.my

G. Manivasagam
Centre for Biomaterials, Cellular and Molecular Theranostics (CBCMT), Vellore Institute of Technology, Vellore, India
e-mail: geethamanivasagam@vit.ac.in

P. S. Bains et al. (eds.), *Biomaterials in Orthopaedics and Bone Regeneration*, Materials Horizons: From Nature to Nanomaterials,
https://doi.org/10.1007/978-981-13-9977-0_5

$u_i/[(L/h_o)(-\mathrm{d}h/\mathrm{d}t)]$ along x direction in parallel plate; $U_i = u_i/[R(\mathrm{d}\varepsilon/\mathrm{d}t)]$ along θ direction in partial journal bearing, $i = 1, 2, 3$

u_j, U_j Fluid velocity at the interface of surface (or porous) layer region I and couple stress fluid film region II, couple stress fluid film region II and surface layer region III, respectively, m/s; $U_j = u_j/[(L/h_o)(-\mathrm{d}h/\mathrm{d}t)]$ along x direction in parallel plate; $U_j = u_j/[R(\mathrm{d}\varepsilon/\mathrm{d}t)]$ along θ direction in partial journal bearing, $j = 12, 23$

w, W Static load, N; $W = wh_0^3/\mu L^3 B(-\mathrm{d}h/\mathrm{d}t)$ for parallel plate; $W = wC^2/\mu R^3 L(\mathrm{d}\varepsilon/\mathrm{d}t)$ for partial journal bearing

x, X X direction coordinate, m; $X = x/L$ for parallel plate; $\theta = x/R$ for partial journal bearing

y, Y Y direction coordinate, m; $Y = y/h_o$ for parallel plate; $Y = y/C$ for partial journal bearing

Greek Letters

δ_i, Δ_i Thickness of surface (or porous) layer region I, couple stress fluid film region II, surface layer region III, respectively, m; $\Delta_i = \delta_i/h_o$ for parallel plate, $\Delta_i = \delta_i/C$ for partial journal bearing; $i = 1, 2, 3$

ε Partial journal bearing eccentricity ratio

μ Core layer (base fluid) viscosity, Ns/m^2 ; $\mu = \mu_2$

μ_i Dynamic viscosity of surface (or porous) layer region I, couple stress fluid film region II, surface layer region III, respectively, Ns/m^2; $i = 1, 2, 3$

β_i Dynamic viscosity ratio of surface (or porous) layer region I to core layer, dynamic viscosity ratio of surface layer region III to core layer, respectively; $\beta_i = \mu_i/\mu$; $i = 1, 3$

η Couple stress material constant, kgm/s

λ Couple stress parameter; $\lambda = \left(\sqrt{\eta/\mu}\right)/h_o$ for parallel plate, $\lambda = \left(\sqrt{\eta/\mu}\right)/C$ for partial journal bearing

θ Angle measured from the center position in partial journal bearing

1 Squeeze Film Bearing Lubrication in Synovial Joints

Squeeze film lubrication characteristics for synovial joints identified as bearings are influenced by surface and lubricant properties. In squeeze film lubrication, fluid between two lubricated surfaces approaching each other is squeezed out and pressure is built up to support the applied load. The load capacity mostly relies on the pressure field induced by the squeezed fluid velocity caused by the approaching surfaces. There is an increasing focus on research on tribological mechanisms and lubrication of synovial joints applications. Mattei et al. [1] reviewed literature on lubrication and

wear models of hip implants that have been used to investigate the effects of geometric and material parameters. The need for including both lubrication and wear aspects that can help in the development of hip implants is highlighted. Myant and Cann [2] reviewed lubrication models of artificial hip joints and suggested that interfacial film formation is driven by aggregation of synovial fluid proteins in shear flow to high viscosity which is entrained into the contact zone. Boedo and Coots [3] investigated the wear characteristics of a novel squeeze film hip implant design based on geometry coupled with kinematic and load characteristics of the human gait cycle. The squeeze film design employing low modulus elastic elements with high modulus metallic coatings showed a promising alternative to contemporary artificial hip joint designs. Pascau et al. [4] investigated the role of fluid film lubrication in total knee replacement systems during the stance phase of walking under various joint conformity conditions. The hydrodynamic lubrication at the early stance phase, coupled with high conformity, helps to decrease significantly the compressive stresses. The synovial joint lubrication investigations are significant in design of total knee replacement (TKR) with large variations in conformity and total hip replacement (THR) based on significant conformity.

This study aims to explore layered squeeze film parallel plate and partial journal bearing described through porous–surface adsorbent layers with couple stress fluid film core region. The porous–surface adsorbent Newtonian layers are of higher viscosity than couple stress fluid core layer of conventional viscosity.

1.1 Squeeze Film Bearings in Synovial Joints

Ruggiero et al. [5, 6] presented synovial fluid film force for squeeze film lubrication of the human ankle joint using closed-form description. The synovial fluid motion through a porous cartilage matrix is depicted as fluid transport across the layered articular cartilage medium [5]. The couple stress characteristics of synovial fluid and porosity of cartilage matrix are considered in the evaluation of fluid film force acting on the synovial human ankle joint during squeeze motion [6]. Mongkolwongrojn et al. [7] presented transient investigation of artificial knee joint in elasto-hydrodynamic lubrication for point contact with non-Newtonian lubricants. Under similar operating conditions, the minimum film thickness obtained for a shear thinning non-Newtonian fluid is lower than a Newtonian fluid. Bujurke and Kudenatti [8] presented squeeze film behavior of poroelastic bearings considering surface roughness of cartilage and couple stress behavior of synovial fluid. Abdullah et al. [9] investigated surface roughness and hydrodynamic lubrication impact on the performance of articular cartilage of synovial human knee joint while gait cycle. Sinha et al. [10] analyzed behavior of synovial fluid lubrication of human joints governed by micro-polar fluid theory. Synovial fluid contains long-chain hyaluronic acid chain molecules causes an increase in the effective viscosity near the porous cartilage, by way of an increase in the micro-motions and the couple stress.

1.1.1 Parallel Plate

Lin et al. [11] investigated the performance of two parallel squeeze film plates considering non-Newtonian couple stresses and convective fluid inertia forces. Combined response of surface quality as well as couple stress fluid in squeeze film poroelastic bearings of synovial joints was investigated by Bujurke et al. [12]. The effects of surface quality and elasticity are more prominent for poroelastic bearings with couple stress fluids.

1.1.2 Partial Journal Bearing

Walicki and Walicka [13] investigated an enhancement in couple stress fluid squeeze film behavior of a synovial joint using hemispherical bearing. Lin [14] predicted the performance of infinitely long partial journal bearing considering the couple stress fluid squeeze film.

1.2 Couple Stress Fluids

The long-chain molecules as polar additives in synovial fluid are characterized as couple stress fluids. Stokes [15] couple stress fluid model derived based on microcontinuum theory is the simplest generalization of the classical theory of fluids. The effect of couple stresses might be expected to appear to a noticeable extent in lubricants containing additives with long-chain molecules. Stokes couple stress fluid model allows for the polar effects such as the presence of couple stresses and body couples. The effects of couple stresses on the squeeze film motion of the synovial joints were analyzed. These investigations on the presence of couple stresses in synovial fluids have led to the enhancement in the load carrying capacity of joints in comparison with the Newtonian lubricant case.

1.3 Layered Lubrication Analysis

The additives have proved to improve the performance of thin film hydrodynamic lubricated contacts forming a thin porous layer adhering to bearing surfaces.

1.3.1 Porous Layer

Many researchers have considered the effects of porosity [16] of cartilage surfaces of the synovial joints. Li and Chu [17] and Elsharkawy [18] presented the effect of porous adsorbent layers and couple stress fluid core layer for improvement in thin

film lubrication performance of journal bearing. To investigate the effects of lubricant additives, the boundary layer microstructure of lubricating surfaces are modeled as thin porous films adsorbed on bearing surfaces. The Brinkman model is used to analyze flow in the porous region and Stokes micro-continuum theory is utilized to model the couple stress effects. Rao et al. [19] presented an analysis of journal bearing with double-layered porous adsorbent film on bearing surfaces with couple stress fluid. The surface layer is simulated as a porous layer with infinite permeability. A low-permeability porous layer interface with core conventional viscosity layer in a lubricant film with double-layered porous layer configuration improves journal bearing performance characteristics.

1.3.2 Surface Layer

Tichy [20] derived generalized Reynolds equation using surface layer model wherein, surface layers possessed higher viscosity than core layer which is pertinent to thin film lubrication. With an increase in thickness and viscosity of surface layers, higher load capacity and lower coefficient of friction are obtained for journal bearing. Szeri [21] investigated significant savings in journal bearing power loss due to reduction in viscous friction based on a structure of a composite film that combines high- and low-viscosity fluids. Rao et al. [22] evaluated three-layered film journal bearing for improvement in load capacity and decline in friction coefficient lubricated with nanoparticle mixed couple stress fluid.

2 Parallel Plate Layered Lubrication with Couple Stress Fluids

This study investigates adsorbent layered couple stress squeeze film lubrication in parallel plate. Figure 1 shows parallel plate with layered lubrication. An adsorbent layered lubrication with couple stress fluid film core region is described through the

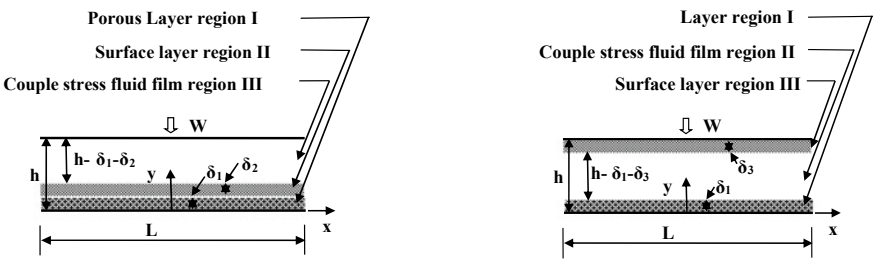

(a) Porous surface double layer

(b) Porous (or surface) – surface layer

Fig. 1 Parallel plate with layered lubrication

following configurations: (i) porous–surface adsorbent double layers (I, II) on stationary plate (Fig. 1a), (ii) porous–surface adsorbent layer (I, III) on stationary–moving plate (Fig. 1b), and (iii) surface–surface adsorbent layer (I, III) on stationary–moving plate (Fig. 1b). The fluid viscosity in the porous layer is considered as conventional core layer viscosity while the surface adsorbent layer viscosity is considered higher than conventional core layer viscosity. A one-dimensional modified Reynolds equation is derived based on Newtonian fluid model in surface layer region, Brinkman model in porous layer region and Stokes model in couple stress fluid film region. The non-dimensional film thickness in layered parallel plate is H. The variation of squeeze film pressure across the layered fluid film is assumed to be negligible. The thickness of surface (or porous) adsorbent layers is considered as constant. Rao et al. [23] analyzed the squeeze film load capacity characteristics of three-layered parallel plate lubricated with couple stress fluids for skeletal joint applications using one-dimensional analysis.

2.1 Porous–Surface Double-Layer Parallel Plate

The momentum equations for porous layer (region I: $0 \le y \le \delta_1$), Newtonian surface layer (region II: $\delta_1 \le y \le \delta_1 + \delta_2$), and the equations of motion for Stokes' couple stress fluid film (region III: $\delta_1 + \delta_2 \le y \le h$) based on thin film lubrication theory are

$$\frac{1}{\mu_1}\frac{\mathrm{d}p}{\mathrm{d}x} = -\frac{u_1}{K_1} + \frac{\mathrm{d}^2 u_1}{\mathrm{d}y^2} \tag{1}$$

$$\frac{1}{\mu_2}\frac{\mathrm{d}p}{\mathrm{d}x} = \frac{\mathrm{d}^2 u_2}{\mathrm{d}y^2} \tag{2}$$

$$\frac{1}{\eta}\frac{\mathrm{d}p}{\mathrm{d}x} = \frac{\mu_3}{\eta}\frac{\mathrm{d}^2 u_3}{\mathrm{d}y^2} - \frac{\mathrm{d}^4 u_3}{\mathrm{d}y^4} \tag{3}$$

The boundary conditions for velocity at the stationary plate, at the interface of stationary plate adsorbent porous and surface layer, at the interface of surface and core couple stress film, and at moving plate, respectively, are

$$y = 0 : u_1 = 0 \tag{4}$$

$$y = \delta_1 : u_1 = u_2 = u_{12}, \quad \mu_1 \frac{\mathrm{d}u_1}{\mathrm{d}y} = \mu_2 \frac{\mathrm{d}u_2}{\mathrm{d}y} \tag{5}$$

$$y = \delta_1 + \delta_2 : u_2 = u_3 = u_{23}, \quad \mu_2 \frac{\mathrm{d}u_2}{\mathrm{d}y} = \mu_3 \frac{\mathrm{d}u_3}{\mathrm{d}y}, \frac{\mathrm{d}^2 u_3}{\mathrm{d}y^2} = 0 \tag{6}$$

$$y = h : u_3 = 0, \quad \frac{\mathrm{d}^2 u_3}{\mathrm{d}y^2} = 0 \tag{7}$$

Integrating Eq. (1) for porous layer ($0 \le Y \le \Delta_1$), Eq. (2) for surface layer ($\Delta_1 \le Y \le \Delta_1 + \Delta_2$), and Eq. (3) for couple stress fluid film ($\Delta_1 + \Delta_2 \le Y \le H$) using the boundary conditions in (4)–(7), the non-dimensional fluid velocity distribution in porous layer ($0 \le Y \le \Delta_1$), surface layer ($\Delta_1 \le Y \le \Delta_1 + \Delta_2$), and couple stress fluid film ($\Delta_1 + \Delta_2 \le Y \le H$) are expressed as

$$0 \le Y \le \Delta_1 : U_1 = U_{12} \frac{\sinh\left(\frac{Y}{\sqrt{K_1}}\right)}{\sinh\left(\frac{\Delta_1}{\sqrt{K_1}}\right)} - K_1 \frac{\mathrm{d}P}{\mathrm{d}X} C_1 \tag{8}$$

$$\Delta_1 \le Y \le \Delta_1 + \Delta_2 : U_2 = \frac{1}{2\beta_2} \frac{\mathrm{d}P}{\mathrm{d}X} (Y - \Delta_1)(Y - \Delta_1 - \Delta_2) - U_{12}\left(\frac{Y - \Delta_1 - \Delta_2}{\Delta_2}\right) + U_{23}\left(\frac{Y - \Delta_1}{\Delta_2}\right) \tag{9}$$

$$\Delta_1 + \Delta_2 \le Y \le H : U_3 = -U_{23}\left(\frac{Y - H}{H - \Delta_1 - \Delta_2}\right) + \frac{1}{2}\frac{\mathrm{d}P}{\mathrm{d}X}(Y - H)(H - \Delta_1 - \Delta_2) + \lambda^2 \frac{\mathrm{d}P}{\mathrm{d}X} C_2 \tag{10}$$

where the coefficients are derived as

$$C_1 = 1 - \frac{\sinh\left(\frac{Y}{\sqrt{K_1}}\right)}{\sinh\left(\frac{\Delta_1}{\sqrt{K_1}}\right)} + \frac{\sinh\left(\frac{Y-\Delta_1}{\sqrt{K_1}}\right)}{\sinh\left(\frac{\Delta_1}{\sqrt{K_1}}\right)},$$

$$C_2 = 1 + \frac{\sinh\left(\frac{Y-H}{\lambda}\right) - \sinh\left(\frac{Y-\Delta_1-\Delta_2}{\lambda}\right)}{\sinh\left(\frac{H-\Delta_1-\Delta_2}{\lambda}\right)} \tag{11}$$

$$U_{12} = -\frac{\mathrm{d}P}{\mathrm{d}X} I_1, \quad U_{23} = -\frac{\mathrm{d}P}{\mathrm{d}X} I_2 \tag{12}$$

$$I_1 = \frac{E_{22}E_{13} - E_{12}E_{23}}{E_{11}E_{22} - E_{12}E_{21}}, \quad I_2 = \frac{-E_{21}E_{13} + E_{11}E_{23}}{E_{11}E_{22} - E_{12}E_{21}} \tag{13}$$

$$E_{11} = \frac{1}{\sqrt{K_1}} \coth\left(\frac{\Delta_1}{\sqrt{K_1}}\right) + \frac{\beta_2}{\Delta_2},$$

$$E_{12} = E_{21} = -\frac{\beta_2}{\Delta_2},$$

$$E_{22} = \frac{\beta_2}{\Delta_2} + \frac{1}{(H - \Delta_1 - \Delta_2)},$$

$$E_{13} = H_1^* + \frac{\Delta_2}{2}, \quad E_{23} = -\lambda H^* + \frac{1}{2}(H - \Delta_1)$$

$$H_1^* = \sqrt{K_1}\left[\coth\left(\frac{\Delta_1}{\sqrt{K_1}}\right) - \operatorname{csch}\left(\frac{\Delta_1}{\sqrt{K_1}}\right)\right]$$
$$H^* = \left[\coth\left(\frac{H-\Delta_1-\Delta_2}{\lambda}\right) - \operatorname{csch}\left(\frac{H-\Delta_1-\Delta_2}{\lambda}\right)\right] \tag{14}$$

The continuity equation across the film in non-dimensional form is

$$Q = \int_0^{\Delta_1} U_1 \mathrm{d}Y + \int_{\Delta_1}^{H-\Delta_3} U_2 \mathrm{d}Y + \int_{H-\Delta_3}^{H} U_3 \mathrm{d}Y, \quad Q = -G\frac{\mathrm{d}P}{\mathrm{d}X} \tag{15}$$

where the coefficient of continuity across the film yields

$$G = I_1\left(H_1^* + \frac{\Delta_2}{2}\right) + K_1\left(\Delta_1 - 2H_1^*\right) + \frac{1}{2}I_2(H-\Delta_1)$$
$$+ \frac{1}{12}\left((H-\Delta_1-\Delta_2)^3 + \frac{\Delta_2^3}{\beta_2}\right) - \lambda^2(H-\Delta_1-\Delta_2) + 2\lambda^3 H^* \tag{16}$$

For $\Delta_2 = 0$, G in Eq. (16) reduces to

$$G = \frac{E_{13}}{E_{11}}\left(H_1^* + \frac{1}{2}(H-\Delta_1)\right) + K_1\left(\Delta_1 - 2H_1^*\right)$$
$$+ \frac{1}{12}(H-\Delta_1)^3 - \lambda^2(H-\Delta_1) + 2\lambda^3 H^* \tag{17}$$

where the coefficients are shown in Eq. (18).

$$E_{11} = \frac{1}{\sqrt{K_1}}\coth\left(\frac{\Delta_1}{\sqrt{K_1}}\right) + \frac{1}{(H-\Delta_1)},$$
$$E_{13} = H_1^* - \lambda H^* + \frac{1}{2}(H-\Delta_1)$$
$$H^* = \left[\coth\left(\frac{H-\Delta_1}{\lambda}\right) - \operatorname{csch}\left(\frac{H-\Delta_1}{\lambda}\right)\right] \tag{18}$$

For $\Delta_1 = 0$, G in Eq. (16) reduces to

$$G = \frac{1}{2}\frac{E_{13}}{E_{11}}H + \frac{1}{12}\left((H-\Delta_2)^3 + \frac{\Delta_2^3}{\beta_2}\right) - \lambda^2(H-\Delta_2) + 2\lambda^3 H^* \tag{19}$$

where the coefficients are

$$E_{11} = \frac{\beta_2}{\Delta_2} + \frac{1}{(H-\Delta_2)}, \quad E_{13} = -\lambda H^* + \frac{1}{2}H,$$

$$H^* = \left[\coth\left(\frac{H-\Delta_2}{\lambda}\right) - \operatorname{csch}\left(\frac{H-\Delta_2}{\lambda}\right)\right] \tag{20}$$

For $\Delta_1 = 0$ and $\Delta_2 = 0$, G in Eq. (16) reduces to

$$G = \frac{1}{12}H^3 - \lambda^2 H + 2\lambda^3 H^* \tag{21}$$

The non-dimensional modified Reynolds equation for squeeze motion is expressed as

$$-1 + \frac{\mathrm{d}Q}{\mathrm{d}X} = 0 \tag{22}$$

The squeeze film boundary conditions are

$$\left.\frac{\mathrm{d}P}{\mathrm{d}X}\right|_{X=0} = 0, \quad P|_{X=\pm 0.5} = 0 \tag{23}$$

Integrating the Eq. (22) and substituting the boundary conditions in Eq. (23), the non-dimensional squeeze film pressure and load capacity in layered parallel plate are derived as

$$P = -\int_{-0.5}^{X} \frac{X}{G}\mathrm{d}X, \quad W = \int_{-0.5}^{0.5} P\mathrm{d}X \tag{24}$$

The parameters employed to investigate outcome of non-dimensional squeeze film load capacity (W) of porous–surface double-layer parallel plate are: non-dimensional film thickness of parallel plate (H) = 0.5–0.9; couple stress parameter (λ) = 0.0–0.2; porous–surface adsorbent double-layer thickness ratios (Δ_1) = 0.0–0.12; (Δ_2) = 0.08; non-dimensional permeability of porous layer (K_1) = 10^{-1}–10^{-5}; and dynamic viscosity ratio of surface to core layer (β_2) = 10. The impact of non-dimensional thickness of porous layer (Δ_1) and non-dimensional-film thickness of parallel plate (H) on the squeeze film non-dimensional load capacity enhancement are analyzed.

Figure 2a, b illustrate the non-dimensional load capacity (W) of parallel plate with porous–surface double layer. The non-dimensional load capacity (W) increases with increase in the non-dimensional thickness of porous layer (Δ_1) and decrease in the non-dimensional film thickness of parallel plate (H). Higher couple stress parameter ($\lambda = 0.2$) and lower non-dimensional permeability ($K_1 = 10^{-5}$) have a significant effect on the increase in non-dimensional load capacity (W) compared to higher non-dimensional permeability ($K_1 = 10^{-1}$). The decline in the non-dimensional permeability of porous layer increases resistance for fluid flow in porous layer.

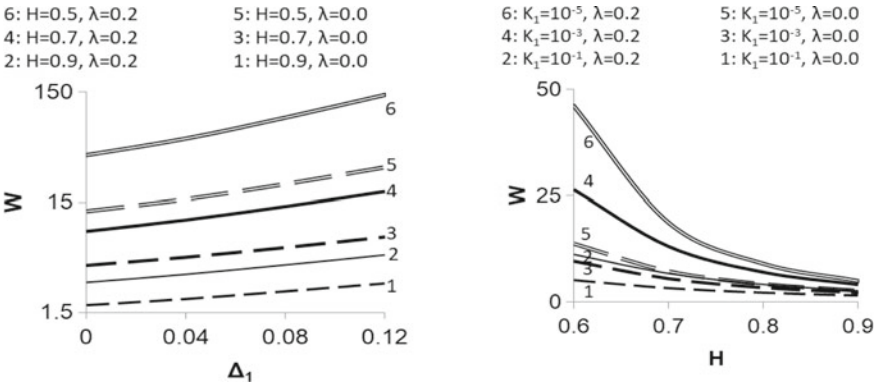

(a) K_1=10^{-5}, β_2=10, Δ_2=0.08 (b) β_2=10, Δ_1=0.12, Δ_2=0.08

Fig. 2 Non-dimensional load capacity of porous surface double-layer parallel plate

2.2 *Porous–Surface Layer Parallel Plate*

The coefficient of continuity across the film in porous– surface layer parallel plate used in determination of non-dimensional squeeze film pressure and load capacity is derived as [22]

$$G = I_1\left(H_1^* + \frac{1}{2}(H-\Delta_1-\Delta_3)\right) + K_1\left(\Delta_1 - 2H_1^*\right) + \frac{1}{2}I_2(H-\Delta_1) + \frac{1}{12}\left((H-\Delta_1-\Delta_3)^3 + \frac{\Delta_3^3}{\beta_3}\right) - \lambda^2(H-\Delta_1-\Delta_3) + 2\lambda^3 H^* \tag{25}$$

where the coefficients are

$$I_1 = \frac{E_{22}E_{13} - E_{12}E_{23}}{E_{11}E_{22} - E_{12}E_{21}}, \quad I_2 = \frac{-E_{21}E_{13} + E_{11}E_{23}}{E_{11}E_{22} - E_{12}E_{21}} \tag{26}$$

$$E_{11} = \frac{1}{\sqrt{K_1}}\coth\left(\frac{\Delta_1}{\sqrt{K_1}}\right) + \frac{1}{(H-\Delta_1-\Delta_3)},$$

$$E_{12} = E_{21} = -\frac{1}{(H-\Delta_1-\Delta_3)},$$

$$E_{22} = \frac{\beta_3}{\Delta_3} + \frac{1}{(H-\Delta_1-\Delta_3)},$$

$$E_{13} = H_1^* - \lambda H^* + \frac{1}{2}(H-\Delta_1-\Delta_3), \quad E_{23} = -\lambda H^* + \frac{1}{2}(H-\Delta_1)$$

$$H_1^* = \sqrt{K_1}\left[\coth\left(\frac{\Delta_1}{\sqrt{K_1}}\right) - \operatorname{csch}\left(\frac{\Delta_1}{\sqrt{K_1}}\right)\right]$$

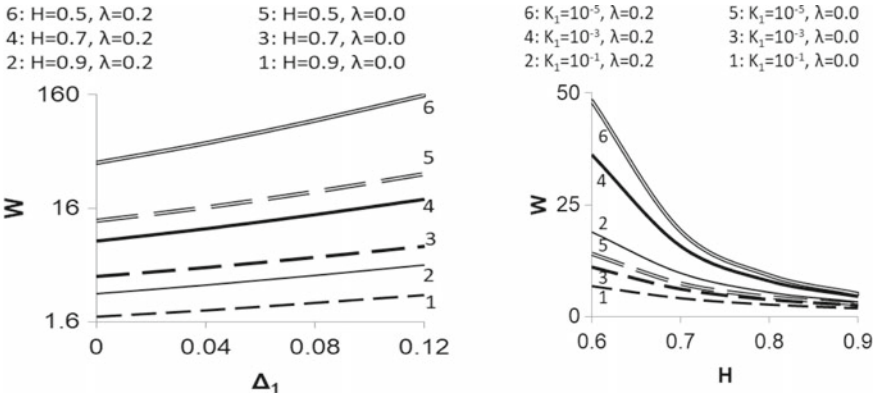

(a) K_1=10^{-5}, β_3=10, Δ_3=0.08 (b) β_3=10, Δ_1=0.12, Δ_3=0.08

Fig. 3 Non-dimensional load capacity of porous–surface layer parallel plate

$$H^* = \left[\coth\left(\frac{H - \Delta_1 - \Delta_3}{\lambda}\right) - \operatorname{csch}\left(\frac{H - \Delta_1 - \Delta_3}{\lambda}\right)\right] \tag{27}$$

The factors employed to examine results of non-dimensional squeeze film load capacity (W) of porous–surface layer parallel plate are: non-dimensional film thickness of parallel plate (H) = 0.5–0.9; couple stress parameter (λ) = 0.0–0.2; porous–surface adsorbent layer thickness ratios (Δ_1) = 0.0–0.12; (Δ_3) = 0.08; non-dimensional permeability of porous layer (K_1) = 10^{-1}–10^{-5}; and ratio of dynamic viscosity of surface to core layer (β_3) = 10. The influence of non-dimensional thickness of porous layer (Δ_1) and non-dimensional film thickness of parallel plate (H) on the squeeze film non-dimensional load capacity enhancement are analyzed.

The influence of porous–surface film parallel plate is investigated in Fig. 3a, b. Similar to Fig. 2a, b at lower non-dimensional permeability ($K_1 = 10^{-5}$), the non-dimensional load capacity (W) increases with increase in the non-dimensional thickness of porous layer (Δ_1) and decrease in non-dimensional film thickness of parallel plate (H) with couple stress fluid core layer ($\lambda = 0.2$). Lower non-dimensional permeability ($K_1 = 10^{-5}$) with couple stress fluid core layer ($\lambda = 0.2$) has a crucial impact on the rise in non-dimensional load capacity (W) than higher non-dimensional permeability ($K_1 = 10^{-1}$).

2.3 Surface–Surface Layer Parallel Plate

The coefficients of continuity across the film in surface–surface layer parallel plate used in determination of non-dimensional squeeze film pressure and load capacity is derived as [22]

$$G = \frac{1}{2}I_1(H-\Delta_3) + \frac{1}{2}I_2(H-\Delta_1) + \frac{1}{12}\left(\frac{\Delta_1^3}{\beta_1} + (H-\Delta_1-\Delta_3)^3 + \frac{\Delta_3^3}{\beta_3}\right) - \lambda^2(H-\Delta_1-\Delta_3) + 2\lambda^3 H^* \quad (28)$$

where the coefficients are

$$E_{11} = \frac{\beta_1}{\Delta_1} + \frac{1}{(H-\Delta_1-\Delta_3)}, \quad E_{13} = -\lambda H^* + \frac{1}{2}(H-\Delta_3) \quad (29)$$

The coefficients I_1, I_2, $E_{12} = E_{21}$, E_{22}, E_{23}, H^* described in Eqs. (26)–(27) are considered in the analysis.

The parameters used to analyze results of non-dimensional squeeze film load capacity (W) of surface–surface layer parallel plate are: non-dimensional film thickness of parallel plate (H) = 0.5–0.9; couple stress parameter (λ) = 0.0–0.2; surface—surface adsorbent layer thickness ratios (Δ_1) = 0.0–0.12; (Δ_3) = 0.08; and dynamic viscosity ratios of surface to core layers (β_1) = 2, 5, 10; (β_3) = 10.

The influence of non-dimensional thickness of surface layer (Δ_1) and non-dimensional film thickness of parallel plate (H) on the squeeze film non-dimensional load capacity enhancement are analyzed in Fig. 4a, b. The non-dimensional load capacity (W) increases with increasing non-dimensional thickness of surface layer (Δ_1 = 0.0–0.12) and decreasing non-dimensional film thickness of parallel plate (H = 0.9–0.5) for couple stress fluids (λ = 0.2). The non-dimensional load capacity (W) increases with decreasing non-dimensional film thickness of parallel plate (H) and increasing dynamic viscosity ratio of surface layer to core layer (β_1 = 2–10). The non-dimensional load capacity (W) increases with increasing squeeze film pressure. Augmented non-dimensional load capacity (W) is achieved with higher

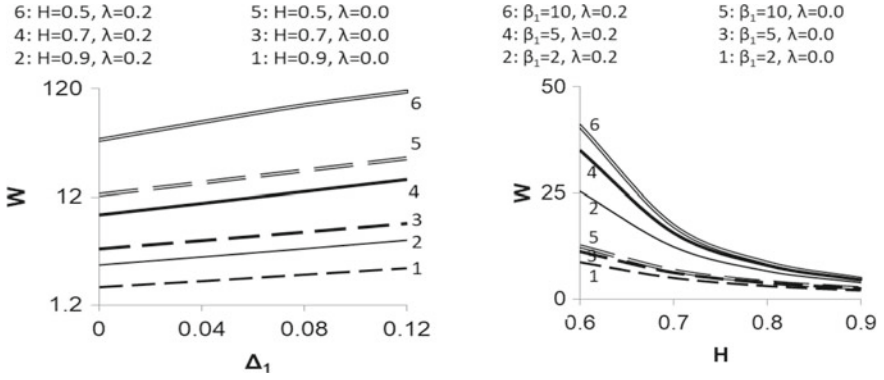

(a) β_1=10, β_3=10, Δ_3=0.08 (b) β_3=10, Δ_1=0.12, Δ_3=0.08

Fig. 4 Non-dimensional load capacity of surface–surface layer parallel plate

non-dimensional surface layer thickness ($\Delta_1 = 0.12$) and lower non-dimensional film thickness of parallel plate ($H = 0.6$) for couple stress fluids ($\lambda = 0.2$).

3 Partial Journal Bearing Layered Lubrication with Couple Stress Fluids

This study investigates adsorbent layered couple stress squeeze film lubrication in partial journal bearing. Figure 5 shows an adsorbent layered lubrication in partial journal bearing with couple stress fluid film core region described through the following configurations: (i) porous–surface adsorbent double layers (I, II) on stationary plate (Fig. 5a), (ii) porous–surface adsorbent layer (I, III) on stationary–moving plate (Fig. 5b), and (iii) surface–surface adsorbent layer (I, III) on stationary–moving plate (Fig. 5b). The fluid viscosity in porous layer is considered as conventional core layer viscosity while the surface adsorbent layer viscosity is considered higher than conventional core layer viscosity. The thickness of porous (or surface) adsorbent layers is considered as constant. Squeeze film non-dimensional load capacity of couple stress fluid lubricated layered partial journal bearing is presented. Rao et al. [21] analyzed the squeeze film load capacity characteristics of three-layered partial journal bearing lubricated with couple stress fluids using one-dimensional analysis.

3.1 Porous–Surface Double-Layer Partial Journal Bearing

The non-dimensional squeeze film pressure and load capacity in layered partial journal bearing are obtained as

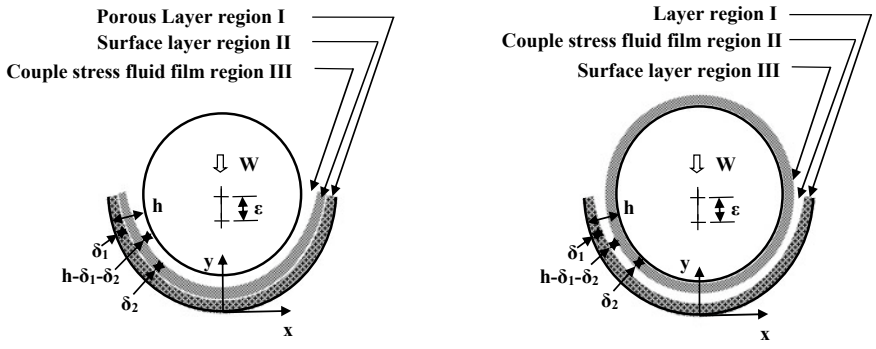

(a) Porous surface double layer

(b) Porous (or surface) – surface layer

Fig. 5 Partial journal bearing with layered lubrication

$$P = -\int_{-0.5\pi}^{\theta} \frac{\sin\theta}{G} \mathrm{d}\theta, \quad W = \int_{-0.5\pi}^{0.5\pi} P\cos\theta \mathrm{d}\theta \tag{30}$$

The coefficients of continuity across the film derived in Eq. (16) for porous–surface double-layer partial journal bearing is used in the analysis. The non-dimensional film thickness in layered partial journal bearing is $H = 1 - \varepsilon\cos\theta$.

The parameters used to analyze the results of non-dimensional squeeze film load capacity (W) of porous–surface double-layer partial journal bearing are: partial journal bearing eccentricity ratio (ε) = 0.1–0.5; couple stress parameter (λ) = 0.0–0.2; porous–surface adsorbent double-layer thickness ratios (Δ_1) = 0.0–0.12; (Δ_2) = 0.08; non-dimensional permeability of porous layer (K_1) = 10^{-1}–10^{-5}; and dynamic viscosity ratio of surface to core layer (β_2) = 10. The influence of non-dimensional thickness of porous layer (Δ_1) and partial journal bearing eccentricity ratio (ε) on the squeeze film non-dimensional load capacity enhancement are analyzed.

Figure 6a, b show the non-dimensional load capacity (W) of partial journal bearing with porous–surface double-layer configuration lubricated with couple stress fluids. The non-dimensional load capacity (W) increases with increasing porous adsorbent layer thickness ratio ($\Delta_1 = 0.0$–0.12) and increasing eccentricity ratio ($\varepsilon = 0.1$–0.5). The resistance to fluid flow in porous layer increases for lower non-dimensional permeability parameter ($K_1 = 10^{-5}$). Higher partial journal bearing eccentricity ratio ($\varepsilon = 0.4$) and lower non-dimensional permeability ($K_1 = 10^{-5}$) show significant influence on increase in non-dimensional load capacity (W) with couple stress fluid core layer ($\lambda = 0.2$).

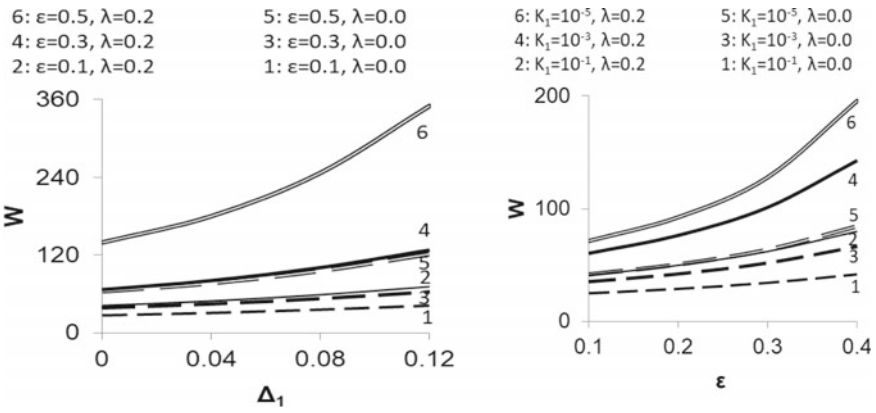

(a) K_1=10^{-5}, β_2=10, Δ_2=0.08 (b) β_2=10, Δ_1=0.12, Δ_2=0.08

Fig. 6 Non-dimensional load capacity of porous–surface double-layer partial journal bearing

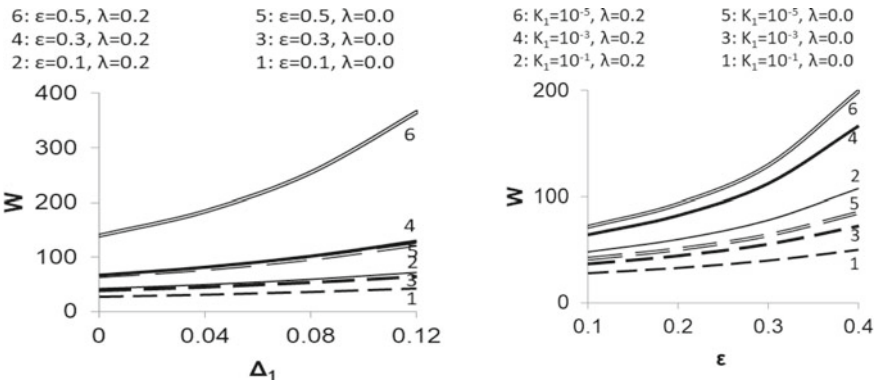

(a) K_1=10^{-5}, β_3=10, Δ_3=0.08 (b) β_3=10, Δ_1=0.12, Δ_3=0.08

Fig. 7 Non-dimensional load capacity of porous–surface layer partial journal bearing

3.2 Porous–Surface Layer Partial Journal Bearing

The parameters used to analyze results of non-dimensional squeeze film load capacity (W) of porous–surface layer partial journal bearing are: partial journal bearing eccentricity ratio (ε) = 0.1–0.5; couple stress parameter (λ) = 0.0–0.2; porous–surface adsorbent layer thickness ratios (Δ_1) = 0.0–0.12; (Δ_3) = 0.08; non-dimensional permeability of porous layer (K_1) = 10^{-1}–10^{-5}; and dynamic viscosity ratio of surface to core layer (β_3) = 10. The influence of non-dimensional thickness of porous layer (Δ_1) and partial journal bearing eccentricity ratio (ε) on the squeeze film non-dimensional load capacity enhancement are analyzed.

The influence of porous–surface film partial journal bearing is investigated in Fig. 7a, b. The variation of non-dimensional load capacity (W) with increasing non-dimensional thickness of porous layer (Δ_1) and increasing partial journal bearing eccentricity ratio (ε) is presented. The non-dimensional load capacity (W) increases with increase in the non-dimensional thickness of porous layer (Δ_1 = 0.0–0.12) at lower non-dimensional permeability of porous layer (K_1 = 10^{-5}). Higher partial journal bearing eccentricity ratio (ε = 0.4), higher non-dimensional thickness of porous layer (Δ_1 = 0.12), and lower non-dimensional permeability (K_1 = 10^{-5}) have significant effect on increase in non-dimensional load capacity (W) for couple stress fluids (λ = 0.2).

3.3 Surface–Surface Layer Partial Journal Bearing

The parameters used to analyze results of non-dimensional squeeze film load capacity (W) of surface–surface layer partial journal bearing are: partial journal bearing

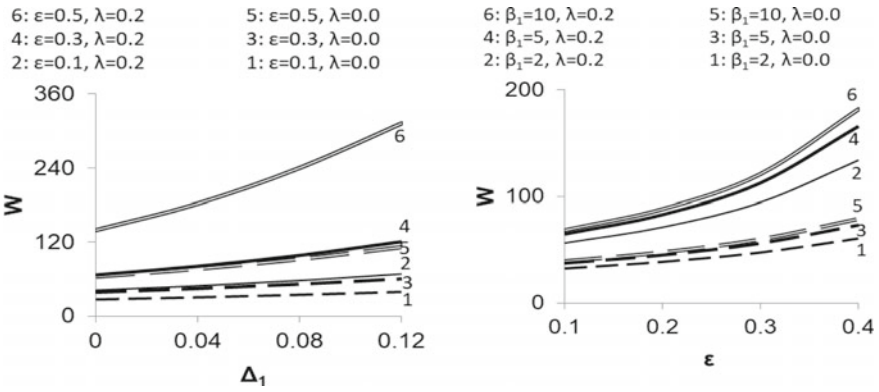

(a) β_1=10, β_3=10, Δ_3=0.08 (b) β_3=10, Δ_1=0.12, Δ_3=0.08

Fig. 8 Non-dimensional load capacity of surface–surface layer partial journal bearing

eccentricity ratio (ε) = 0.1–0.5; couple stress parameter (λ) = 0.0–0.2; surface–surface adsorbent layer thickness ratios (Δ_1) = 0.0–0.12; (Δ_3) = 0.08; and dynamic viscosity ratios of surface to core layers (β_1) = 2, 5, 10; (β_3) = 10.

The influence of non-dimensional thickness of surface layer (Δ_1) and partial journal bearing eccentricity ratio (ε) on the squeeze film non-dimensional load capacity (W) enhancement are analyzed in Fig. 8a, b. The non-dimensional load capacity (W) increases with increase in non-dimensional thickness of surface layer (Δ_1 = 0.0–0.12) for couple stress fluids ($\lambda = 0.2$). The non-dimensional load capacity (W) increases with increasing partial journal bearing eccentricity ratio (ε = 0.1–0.4) for couple stress fluids ($\lambda = 0.2$) with increasing dynamic viscosity ratio of surface layer to core layer (β_1 = 2–10). Higher non-dimensional load capacity (W) is obtained for couple stress fluids ($\lambda = 0.2$) with higher non-dimensional thickness of surface layer ($\Delta_1 = 0.12$) and higher partial journal bearing eccentricity ratio ($\varepsilon = 0.5$).

4 Conclusions

An improvement in squeeze film load capacity of layered parallel plate and partial journal bearing lubricated with couple stress fluids is evaluated using (i) porous–surface double layer, (ii) porous–surface layer, and (iii) surface–surface layer. Adsorbent porous and surface layers are analyzed using permeability and viscosity ratio (surface to core layer) parameters, respectively. Modified Reynolds equation is derived for wide-layered parallel plate and long-layered partial journal bearing based on one-dimensional analysis. Squeeze film boundary conditions are used to solve modified Reynolds equation to determine squeeze film pressure.

The non-dimensional squeeze film load capacity (W) increases significantly with lower non-dimensional permeability of porous layer ($K_1 = 10^{-5}$), higher non-dimensional porous–surface layer thickness ($\Delta_1 = 0.12$), higher dynamic viscosity ratio of surface layer to core layer conventional viscosity ($\beta_1, \beta_2, \beta_3 = 10$), and higher couple stress parameter for core fluid layer ($\lambda = 0.2$).

Higher viscosity and thickness of adsorbent low-permeable porous or surface layers with core couple stress fluid increases the squeeze film load capacity of layered parallel plate and partial journal bearing. Couple stress fluids with adsorbent porous–surface layers enhances load capacity of squeeze film bearings for skeletal joint applications.

References

1. Mattei L, Puccio FD, Piccigallo B, Ciulli E (2011) Lubrication and wear modelling of artificial hip joints: a review. Tribol Int 44:532–549
2. Myant C, Cann P (2014) On the matter of synovial fluid lubrication: implications for metal-on-metal hip tribology. J Mech Behav Biomed Mater 34:338–348
3. Boedo S, Coots SA (2017) Wear characteristics of conventional and squeeze-film artificial hip joints. J Tribol 139(3):031603
4. Pascau A, Guardia B, Puertolas JA, Gomez-Barrena E (2019) Knee model of hydrodynamic lubrication during the gait cycle and the influence of prosthetic joint conformity. J Orthop Sci 14:68–75
5. Ruggiero A, Gomez E, D'Amato R (2011) Approximate analytical model for the squeeze-film lubrication of the human ankle joint with synovial fluid filtrated by articular cartilage. Tribol Lett 41:337–343
6. Ruggiero A, Gomez E, D'Amato R (2013) Approximate closed form solution of the synovial fluid film force in the human ankle joint with non-Newtonian lubricant. Tribol Int 57:156–161
7. Mongkolwongrojn M, Wongseedakaew K, Kennedy FE (2010) Transient elastohydrodynamic lubrication artificial knee joint with non-Newtonian fluids. Tribol Int 43:1017–1026
8. Bujurke NM, Kudenatti RB (2006) An analysis of rough poroelastic bearings with reference to lubrication mechanism of synovial joints. Appl Math Comp 178:309–320
9. Abdullah EY, Edan NM, Kadhim AN (2017) Study surface roughness and friction of synovial human knee joint with using mathematical model, Special issue: 1st Scientific International Conference, College of Science, Al-Nahrain University, 21st–22th November 2017, Part I, pp 109–118
10. Sinha P, Singh C, Prasad KR (1982) Lubrication of human joints—a micro continuum approach. Wear 80:159–181
11. Lin JR, Hung CR, Lu RF (2006) Averaged inertia principle for non-newtonian squeeze films in wide parallel plates: couple stress fluid. J Marine Sci Techonol 14:218–224
12. Bujurke NM, Kudenatti RB, Awati VB (2007) Effect of surface roughness on squeeze film poroelastic bearings with special reference to synovial joints. Math Biosci 209:76–89
13. Walicki E, Walicka A (2000) Mathematical modelling of some biological bearings. Smart Mater Struct 9:280–283
14. Lin JR (1997) Squeeze film characteristics of long partial journal bearings lubricated with couple stress fluids. Tribol Int 30:53–58
15. Stokes VK (1966) Couple stresses in fluids. Phys Fluids 9:1709–1715
16. Bhui AS, Singh G, Sidhu SS, Bains PS (2018) Experimental investigation of optimal ED machining parameters for Ti-6Al-4 V biomaterial. FU Mech Eng 16(3):337–345

17. Li WL, Chu HM (2004) Modified reynolds equation for couple stress fluids—a porous media model. Acta Mech 171:189–202
18. Elsharkawy AA (2005) Effects of lubricant additives on the performance of hydro dynamically lubricated journal bearings. Tribol Lett 18:63–73
19. Rao TVVLN, Rani AMA, Nagarajan T, Hashim FM (2013) Analysis of journal bearing with double-layer porous lubricant film: Influence of surface porous layer configuration. Tribol Trans 56:841–847
20. Tichy JA (1995) A surface layer model for thin film lubrication. Tribol Trans 38(3):577–582
21. Szeri AZ (2010) Composite-film hydrodynamic bearings. Int J Eng Sci 48:1622–1632
22. Rao TVVLN, Sufian S, Mohamed NM (2013) Analysis of nanoparticle additive couple stress fluids in three-layered journal bearing. J Phys Conf Ser 431:012023
23. Rao TVVLN, Rani AMA, Manivasagam G (2018) Squeeze film analysis of three-layered parallel plate and partial journal bearing lubricated with couple stress fluids for skeletal joint applications. Mater Today Proc (Accepted)